BULLETIN OF THE POLISH ACADEMY OF SCIENCES
TECHNICAL SCIENCES, Vol. 71(2), 2023, Article number: e144610
DOI: 10.24425/bpasts.2023.144610

Effect of spray distance on the microstructure and corrosion resistance of WC-based coatings sprayed by HVOF

Ewa JONDA [1]*, Leszek ŁATKA [2], Artur MACIEJ [3], Marcin GODZIERZ [4], Klaudiusz GOŁOMBEK [5], and Andrzej RADZISZEWSKI [6]

[1] Silesian University of Technology, Faculty of Mechanical Engineering, Department of Engineering Materials and Biomaterials, ul. Konarskiego 18a, 44-100 Gliwice, Poland
[2] Wroclaw University of Science and Technology, Faculty of Mechanical Engineering, Department of Metal Forming, Welding and Metrology, ul. Łukasiewicza 5, 50-371 Wroclaw, Poland
[3] Silesian University of Technology, Faculty of Chemistry, Department of Inorganic and Analytical Chemistry and Electrochemistry, ul. Krzywoustego 6B, 44-100 Gliwice, Poland
[4] Polish Academy of Sciences, Centre of Polymer and Carbon Materials, ul. M. Curie-Skłodowskiej 34, 41-819 Zabrze, Poland
[5] Silesian University of Technology, Laboratory of the Testy Materials, Silesian University of Technology, ul. Konarskiego 18a, 44-100 Gliwice, Poland
[6] "RESURS" Company, A. Radziszewski, ul. Czarodzieja 12, 03-116 Warszawa, Poland

Abstract. Cermet coatings provide protection against an aggressive operating environment of machine and device elements, such as corrosion, wear or high-temperature conditions. Currently, WC-based cermet coatings are frequently used in different industry branches. In this work, conventional WC-based powders (WC-Co and WC-Co–Cr) were sprayed with high velocity oxy fuel (HVOF) onto AZ31 magnesium alloy with different spray distances (320 and 400 mm). The research aimed to investigate the effect of the spray distance on the microstructure of the coatings, phase composition and electrochemical corrosion resistance. Results revealed that a higher spray distance results in greater porosity, 1.9% and 2.3% for 320 mm and 2.8% and 3.1% for 400 mm in the case of WC-Co and WC-Co–Cr coatings, respectively. Also, an impact on coatings microhardness was observed, c.a. 1300 HV0.3 for shorter spray distances, whereas for longer ones it was less than 1100 HV0.3. The corrosion resistance estimated in potentiodynamic polarization measurements was the best for WC-Co–Cr coating deposited from the shorter spray distance, corrosion current density was equal to 2.9 $\mu A \cdot cm^{-2}$ and polarization resistance was equal to 8424 $\Omega \cdot cm^2$.

Key words: WC-based powders; AZ31 magnesium alloy; high velocity oxy fuel; microstructure; corrosion resistance.

1. INTRODUCTION

Due to the low value of specific gravity and high specific strength, magnesium alloys are increasingly used in a wide range of industry branches, among others, in automotive, aerospace, chemical, shipbuilding and electronics [1–3]. However, their application is limited by low corrosion-, erosion- and abrasive-wear resistance, as well as low hardness [4–6]. The corrosion mechanism of magnesium alloys depends on the type of alloy, impurities from the production process and the possibilities of its potential applications, among others. [7]. In surface engineering, there are two main methods of improving the corrosion resistance of the surface of magnesium alloys by modifying their properties: physical or chemical techniques [8, 9]. One of them is manufacturing protective and/or regenerative coatings. However, in such a case, special attention should be paid to the problem of the flammability and high plasticity of magnesium alloys [10, 11]. Therefore, it is necessary to select an appropriate technology of surface engineering which allows for the production of a dense, compact and well-adhered coating under relatively low-temperature conditions affecting the substrate [12]. The method in the field of thermal spraying which meets the above requirements is high velocity oxygen fuel (HVOF) spraying [13, 14]. One of the most significant advantages of this method is the possibility to manufacture ceramic, carbide as well as cermet coatings of almost unrestricted chemical and/or phase composition [15–17]. In the area of developing modern techniques of enhancement of the surface properties of machine elements, this method is a good alternative to other methods in the area of thermal spraying and is mainly used to make coatings with high abrasion resistance, as well as high temperature and corrosion resistance [18–20]. Nevertheless, such properties could be achieved only with correctly selected parameters of the thermal spraying process [21, 22]. It is also important that in this scientific area, there is only a small number of papers dealing with research on the production of

*e-mail: ewa.jonda@polsl.pl

Manuscript submitted 2022-09-15, revised 2023-01-05, initially accepted for publication 2023-01-09, published in April 2023.

the above-mentioned coatings deposited on magnesium alloys, and the authors' own research constitutes a certain knowledge base, the aim of which is to fill this gap in the literature [23,24]. Therefore, this paper focuses on the impact of one of the most significant process parameters, the spray distance, on the microstructure and corrosion resistance of the manufactured coatings. The comparison of the two types of cermet materials was also highlighted in the paper.

2. MATERIALS AND METHODS

2.1. Feedstock

In this paper, two commercial powders (from Höganäs) were used, namely:

- Amperit 518.074: WC-12Co (wt.%)
- Amperit 558.074: WC-10Co–4Cr (wt.%)

The delivery state for both powders was agglomerated and sintered. Moreover, the range of particle size declared by the manufacturer was $-45+15$ µm for both feedstocks. The SEM observations confirmed that particles have a spherical shape (Fig. 1) which improves their flowability during thermal spraying.

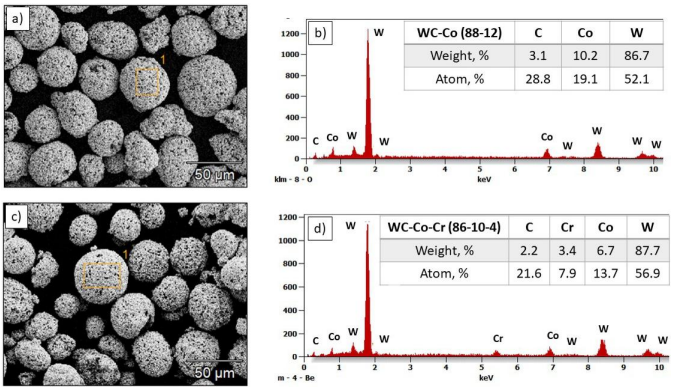

Fig. 1. Morphology of WC-Co (a), and WC-Co–Cr (c), the results of chemical analysis (b) from point (a) and (d) from point (c) of the powders, (SEM)

Moreover, the examination of the average particle size of the powders was performed using Fritisch Analysette 22 Micro Tec plus (Germany). The average particle size of the powders is given in Fig. 2. It can be seen that the average particle size d_{V50} of both used powders is similar ($34-35$ µm).

2.2. Deposition process

In this study, AZ31 magnesium alloy (with 5 mm thickness) was used as a substrate material. Before the deposition process samples were sandblasted (final $R_a = 3.2$ µm) and cleaned with ethanol. A spray system JP 5000 TAFA (Indianapolis, USA) from RESURS (Warsaw, Poland) was employed for the deposition of the coatings. The spray parameters are summarized in Table 1.

In current studies, the variable factor was the spray distance which is one of the key process parameters. The sample code with the values of the variable process parameters is presented in Table 2.

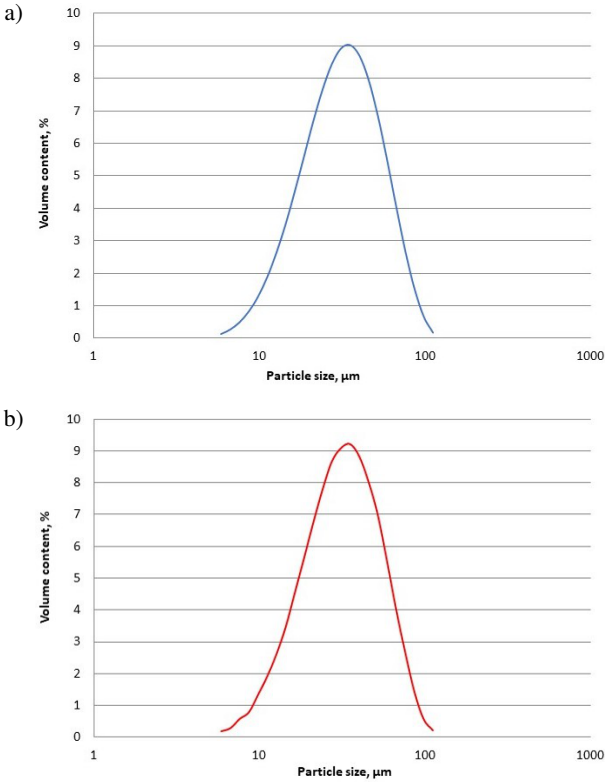

Fig. 2. Particle size distribution of powders used for spraying: WC-Co (a) and WC-Co–Cr (b)

Table 1
Spray parameters

Kerosene (l/h)	26.1
Oxygen (slpm)	900
Nitrogen (slpm)	12
Powder feed rate (g/min)	70
Water flow (slpm)	23

Table 2
The sample code and variable parameter values

The feedstock powder	Spray distance, mm	
	320	400
	Sample code	
WC-Co	C1-D1	C1-D3
WC-Co–Cr	C2-D1	C2-D3

2.3. Characterization of coatings

After HVOF thermal spraying, the standard metallographic procedure was applied. The cross sections of the coated samples were prepared by cutting, embedding in cold mounting resin and then grinding and polishing. Scanning electron microscope with secondary electron and backscattered detectors (Supra 35,

Zeiss, Oberkochen, Germany) was used for microscopic investigations and fracture morphology. The chemical composition was analyzed by EDS (energy dispersive X-ray spectroscopy). The porosity of the coatings was measured by means of an image analysis software ImageJ open coating according to ASTM E2109 – 01 standard. The cross sections of obtained samples were observed by a digital light microscope Keyence VHX6000 (Keyence International, Mechelen, Belgium). Twenty measurements at the magnification of 1000x were carried out at random locations. Then, the average thickness, as well as standard deviation values were calculated.

The X-ray diffraction (XRD) studies were performed using the D8 Advance diffractometer (Bruker, Karlsruhe, Germany) with Cu-Kα cathode ($\lambda = 0.154$ nm). The copper tube was operating at 40 kV voltage and 40 mA current. The samples were examined in the range of 20° to 120°2Θ, with a scanning step of 0.02° and a scan rate of 0.60°/min. Fitted phases were identified using DIFFRAC.EVA program equipped with ICDD PDF#2 database. The exact lattice parameters of the fitted phase were calculated using Rietveld refinement in TOPAS 6 program, using a pseudo-Voigt function in the description of diffraction line profiles. As mathematical factors of calculated for experimental pattern fit, the R_{wp} (weighted-pattern factor) and S (goodness-of-fit) parameters were used.

The surface roughness of the deposited coatings was measured according to the ISO 4288 standard using a profilometer MarSurf PS10 (Mahr, Gottingen, Germany). For each sample, five measurements of R_a and R_z parameters were conducted. Then the average and standard deviation values were calculated.

Vickers microhardness was estimated with the value of maximum load equal to 2.94 N (HV0.3) according to the ISO 4516 standard and was developed to evaluate the hardness of the sprayed coatings. At least ten imprints were conducted on the coating cross-section. The HV-1000 hardness tester (Sinowon Innovation Metrology) was used. The average value of microhardness, as well as the standard deviation, was calculated.

The corrosion resistance investigations of the sprayed AZ31 alloy were realized by the potentiodynamic Tafel method using an AUTOLAB PGSTAT100 potentiostat – galvanostat (Metrohm Autolab BV, The Netherlands). The corrosion resistance assessment was conducted in a 3.5% solution of NaCl at a temperature equal to 25°C. Before the determination of the polarization and open circuit potentials (EOC), all samples were stabilized at a time equal to 3600 s. The measurements of the linear sweep voltammetry (LSV) were estimated at potential values in the range of EOC from −150 mV up to +150 mV. The scan rate was equal to 0.167 mV·s^{-1}. The achieved voltammograms were analyzed by NOVA 2.1 software in order to determine corrosion properties, such as polarization resistance (R_p), corrosion current density (j_{corr}), and corrosion potential (E_{corr}). The electrochemical cell used in the measurements was built in the double-walled (thermostatic) mode with a three-electrode configuration. A saturated calomel electrode (SCE) was used as the reference. Additionally, a platinum mesh was used as the counter electrode. For comparison, analogical measurements were also conducted for not coated AZ31 magnesium alloy.

3. RESULTS AND DISCUSSION

3.1. Microstructure of the coatings

The observations of the coating topography revealed a typical morphology of HVOF-sprayed coatings [25,26]. In general, the surface is relatively smooth, with some irregularity which could be observed (Fig. 3) probably due to the fact that the hard carbide particles did not melt in the flame [27]. Some differences in the surface roughness of manufactured coatings could be observed. It is an effect of the spray distance. Similar dependence – an increasing roughness with elongation of the stand-off distance was observed in [28].

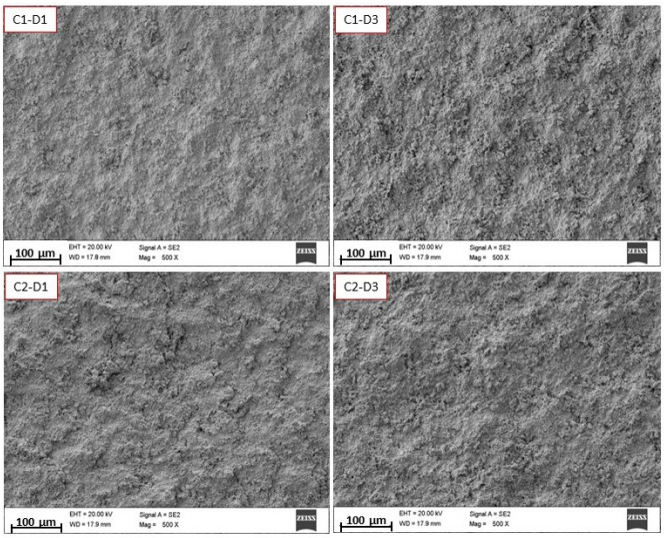

Fig. 3. The topography of the HVOF-sprayed coatings, (SEM)

Based on the microstructure investigations, it was found that the manufactured coatings are characterized by a dense and relatively uniform structure (Fig. 4a) which is characteristic for HVOF process [29–31]. Detailed examination revealed that the porosity level is low, and the pores are fine (much lower than 1 µm). Such fine pores could improve the corrosion resistance of sprayed coatings [32].

a)

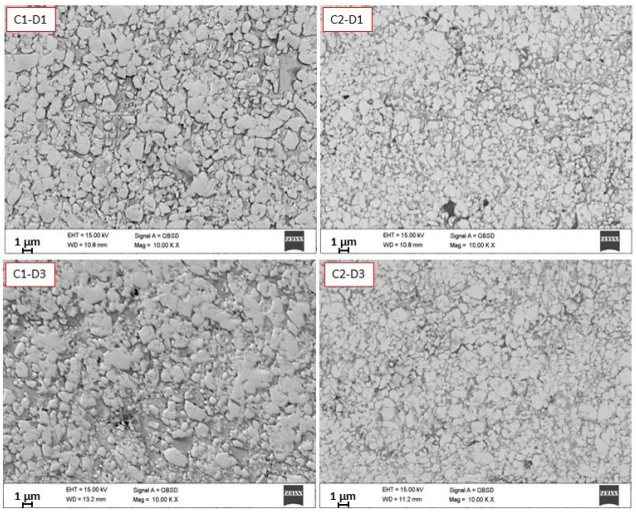

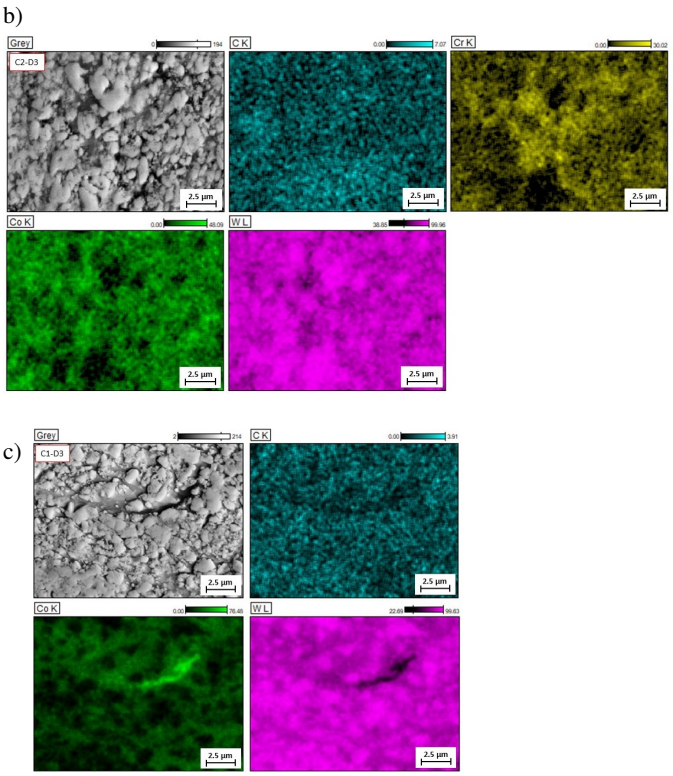

Fig. 4. The microstructure of the HVOF-sprayed coatings: a) middle area of the coating; b), c) elemental distribution maps of elements in the analyzed area, (SEM)

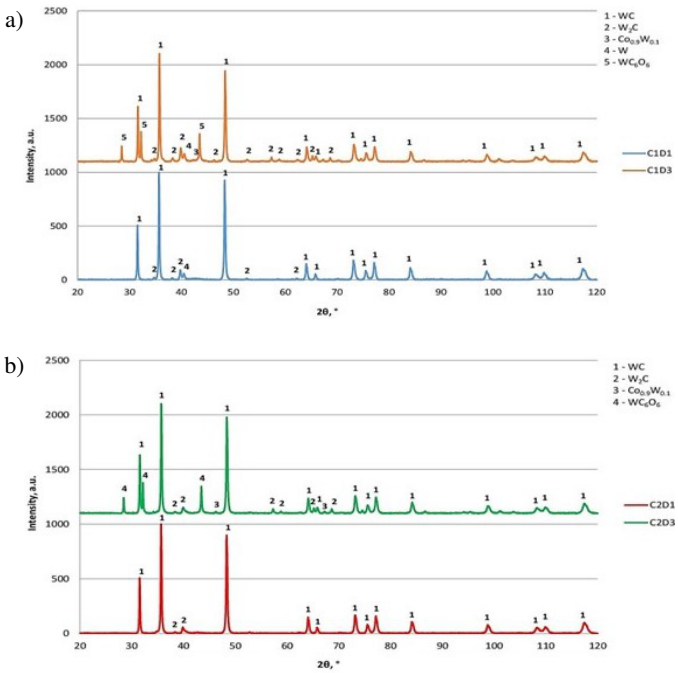

Fig. 5. The phase composition of the HVOF-sprayed coatings (SEM): WC-Co (a) and WC-Co–Cr (b)

Additional analysis of the deposited coatings by EDS and elemental distribution maps confirmed that samples consist of WC particles embedded in a Co or Co–Cr matrix, depending on the used feedstock material. SEM images of the coatings showing unmelted carbide particles in the matrix (Figs. 4b and 4c). Furthermore, their shape clearly shows that they were partially melted during the HVOF spraying process. Similar results could be found in [33]. The average coating thickness ranges from 250 up to 350 µm. On the other hand, there are some material discontinuities that could be seen, especially for longer spray distances, which do not allow us to form a dense structure. Also, the lower content of the cobalt matrix for C2 coatings could have an impact on increasing porosity values [34, 35].

3.2. Phase composition

The phase composition of the manufactured coatings consists of two hexagonal carbides: WC and W_2C, hexagonal Co, and cubic solid solution of tungsten in cobalt with composition $Co_{0.9}W_{0.1}$ [36]. For the longest spray distance (samples C1–D3 and C2–D3) also a small quantity of WC_6O_6 phase has been identified as a consequence of partial oxidation of WC (Fig. 5). Such results were confirmed by [37, 38]. For additional analysis of the phase composition, the index of carbide retention (ICR) was proposed [39]. The obtained results of ICR values for WC-Co samples were equal to 0.91 and 0.92 for C1–D1 and C1–D3, respectively. For WC-Co–Cr samples, ICR values were equal to 0.95 and 0.96 for C2–D1 and C2–D3, respectively. The presence of chromium reduces the tendency of W_2C formation as well as the increasing spray distance [40]. It should be stressed that the ICR value closer to the unity is better in terms of coatings cohesion and wear- and corrosion resistance [41].

3.3. Corrosion resistance

The results of the potentiodynamic investigations revealed that coated samples exhibit much better corrosion resistance than uncoated magnesium alloy AZ31 (Fig. 6) in the environment of sodium chloride solution. A detailed analysis of the potentiodynamic curve indicates that AZ31 alloy in the 3.5% NaCl solution started to oxidize. Such behaviour was observed also in other light material alloys, e.g. [42]. For coated samples, a decrease in the corrosion current density (j_{corr}) and an increase in the corrosion potential (E_{corr}) could be observed. The presence of the cermet coating inhibits anodic processes (more flat curve shape).

The polarization resistance of the magnesium alloy is very low (241.3 $\Omega \cdot cm^2$) whereas the corrosion current density is high (57.4 $\mu A \cdot cm^{-2}$). The corrosion potential of the AZ31 alloy equals –1.56 V, which is characteristic of the magnesium alloy in NaCl solution [43–45]. The manufacturing of the protective coatings on the AZ31 alloy substrate by HVOF led to a significant shift of the corrosion potential towards more positive values. In the specified electrochemical system, all the coatings have a cathodic character and in the case of corrosion cell formation, the magnesium alloy substrate as an anode will corrode first. The biggest change of E_{corr} was registered for the samples C2–D1 and C2–D3 (–0.506 V and –0.579 V, respectively). Also samples C1–D1 and C1–D3 also result in a significant shift of the corrosion potential towards more positive values (–0.690 V and –0.747 V, respectively). Similar values were reported by Utu [46] and Shabana [47].

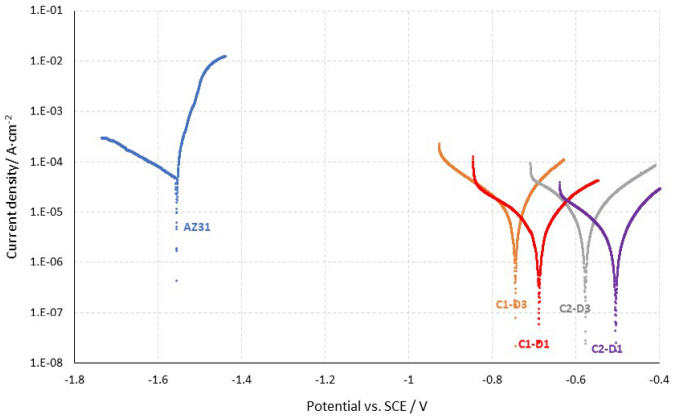

Fig. 6. Potentiodynamic curves for the cermet coatings and uncoated AZ31 as a reference

Similar behaviour of the two types of coatings was noticed in relation to the spray distance. It was noticed that in the case of a shorter distance (320 mm), the corrosion potential values were higher than for the distance of 400 mm. The difference in E_{corr} values in the two types of coatings was similar, i.e. 74 mV (for C1 samples) and 57 mV (for C2 samples). In the case of the coatings formed by using the distance of 320 mm, the polarisation resistance (Rp) values were higher (and corrosion current density values were lower) than for the coatings sprayed by using the distance of 400 mm. It could result from a more compact structure. Such a phenomenon was registered by Hong [48].

It should be stressed that all HVOF sprayed cermet coatings exhibit good protection properties for the magnesium alloy. Nevertheless, the best improvement of corrosion resistance was provided by the C2–D1 sample. This coating was characterized by c.a. 20 times lower corrosion current density ($j_{corr} = 2.9$ μA·cm^{-2}) in comparison to magnesium alloy substrate ($j_{corr} = 57.4$ μA·cm^{-2}). The other coatings have also lower corrosion current density (see Table 3). Similar results could be found in [47, 49, 50].

Additionally, in Table 3 it could be clearly seen that polarization resistance is also even 20 times higher for coated sample (C2–D1) in order to uncoat the AZ31 substrate.

Table 3
The results of the potentiodynamic measurements in 3.5% NaCl solution

Sample code	Corrosion current density (j_{corr}, μA·cm^{-2})	Polarization resistance, R_p (Ω·cm^2)	Corrosion potential (E_{corr}), vs. SCE (V)
AZ31	57.4	241.3	–1.557
C1–D1	3.5	6733	–0.690
C1–D3	11.7	2621	–0.747
C2–D1	2.9	8423	–0.506
C2–D3	7.3	4180	–0.579

3.4. Roughness, porosity and microhardness of deposited coatings

The values of surface roughness and porosity are given in Table 4. The tendency is clearly observed, a shorter spray distance results in lower porosity of the coatings. On the other hand, the porosity depends on many technological parameters, for example, the type and shape of the feedstock powders [51, 52].

In the case of surface roughness, the slight influence of the spray distance could be observed, but the differences are in the range of standard deviation. Such values are typical for standard HVOF cermet coatings [53, 54].

Table 4 also includes the results of microhardness estimation. It was found that the highest value is exhibited by sample C1–D1, whereas the lowest one was characteristic for sample C2–D3. Such results revealed that a shorter spray distance promoted a more compact structure with a lower amount of pores [55, 56].

Table 4
Average values of roughness (R_a, R_z), porosity and microhardness of deposited coatings

Sample code	Roughness parameter (μm)		Porosity (vol.%)	Microhardness HV0.3
	R_a	R_z		
C1–D1	3.81 ± 0.27	22.25 ± 1.86	1.9 ± 0.5	1305 ± 148
C1–D3	3.59 ± 0.24	20.98 ± 1.08	2.8 ± 0.7	1085 ± 176
C2–D1	4.08 ± 0.24	23.30 ± 0.87	2.3 ± 0.5	1278 ± 127
C2–D3	3.82 ± 0.17	22.60 ± 1.50	3.1 ± 0.6	1042 ± 186

4. CONCLUSIONS

In this study, WC-Co and WC-Co–Cr coatings deposited by HVOF thermal spraying from commercially available feedstock powders onto AZ31 magnesium alloy with different spray distances (320 and 400 mm) were inspected in terms of their microstructure, phase composition and electrochemical corrosion resistance. The experimental results can be summarized as follows:

- All manufactured coatings revealed a topography and microstructure typical for the HVOF process, with regular and smooth surfaces as well as a compact structure. Moreover, in the coatings, the carbide distribution is even.
- Investigations of phase composition revealed the presence of hexagonal WC, W_2C and Co as well as a cubic solid solution of tungsten in cobalt ($Co_{0.9}W_{0.1}$). Moreover, for longer spray distances, the small quantity of WC_6O_6 phase was identified as a consequence of partial oxidation of WC.
- The clear influence of the spray distance on corrosion resistance was observed. The j_{corr} values were lower, whereas R_p values were higher for shorter spray distances, which improves corrosion resistance.
- The same influence of the spray distance was also observed in the case of porosity and microhardness. A lower porosity value was connected with better corrosion resistance.

ACKNOWLEDGEMENTS

The financial support of the Ministry of Science and Higher Education of Poland is gratefully acknowledged, grant no. DEC – 2019/03/X/ST5/00830.

REFERENCES

[1] X. Yang *et al.*, "Microstructure and mechanical properties of wire and arc additive manufactured AZ31 magnesium alloy using cold metal transfer process," *Mater. Sci. Eng.* A, vol. 774, pp. 1–9, 2020, doi: 10.1016/j.msea.2020.138942.

[2] Y. Mazaheri, M. Mahdi, J. Akbar, H. Amir, and R. Jahani, "Tribological behavior of AZ31/ZrO_2 surface nanocomposites developed by friction stir processing," *Tribol. Int.*, vol. 143, pp. 1–14, 2020, doi: 10.1016/j.triboint.2019.106062.

[3] Y. Yang, X. Xiong, J. Chen, X. Peng, D. Chen, and F. Pan, "Research advances in magnesium and magnesium alloys worldwide in 2020," *J. Magnes. Alloy.*, vol. 9, pp. 705–747, 2021, doi: 10.1016/J.JMA.2021.04.001.

[4] Y. Fouad and M. El Batanouny, "Effect of surface treatment on wear behavior of magnesium alloy AZ31," *Alex. Eng. J.*, vol. 50, pp. 19–22, 2011, doi: 10.1016/j.aej.2011.01.003.

[5] C. Taltavull, A.J. Lopez, B. Torres, A. Atrens, and J. Rams, "Optimization of the high velocity oxygen fuel (HVOF) parameters to produce effective corrosion control coatings on AZ91 magnesium alloy," *Mater. Corros.*, vol. 66, pp. 423–432, 2015, doi: 10.1002/maco.201407982.

[6] G. Song and Z. Xu, "The surface, microstructure and corrosion of magnesium alloy AZ31 sheet," *Electrochim. Acta*, vol. 55, pp. 4148–4161, 2010, doi: 10.1016/j.electacta.2010.02.068.

[7] G. Song and A. Atrens, "Corrosion mechanisms of magnesium alloys," *Adv. Eng. Mater.*, vol. 1, pp. 11–33, 1999, doi: 10.1002/(SICI)1527-2648(199909)1:1<11::AID-ADEM11>3.0.CO;2-N.

[8] D.K. Dwivedi, "*Surface Engineering. Enhanced Life of Tribological Components*," Springer, 2018.

[9] N. Espallargas, Ed., "*Future Development of Thermal Spray Coatings. Types, Designs, Manufacture and Applications*," Woodhead Publishing, Elsevier, 2015, pp. 1–13, doi: 10.1016/B978-0-85709-769-9.09988-7.

[10] J.F. Nie, "Precipitation and Hardening in Magnesium Alloys," *Metall. Mater. Trans. A*, vol. 43A, pp. 3891–3939, 2012, doi: 10.1007/s11661-012-1217-2.

[11] Q.B. Nguyen, Y.H.M. Sim, M. Gupta, and C.Y.H. Lim, "Tribology characteristics of magnesium alloy AZ31B and its composites," *Tribol. Int.*, vol. 82, pp. 464–471, 2015, doi: 10.1016/j.triboint.2014.02.024.

[12] L. Łatka, L. Pawłowski, M. Winnicki, P. Sokołowski, A. Małachowska, and S. Kozerski, "Review of functionally graded thermal sprayed coatings," *Appl. Sci.*, vol. 10, p. 5153, 2020, doi: 10.3390/app10155153.

[13] L. Pawłowski, "*The Science and Engineering of Thermal Spray Coatings*," John Wiley & Sons, Ldt, England, 2008, pp. 67–113, doi: 10.1002/9780470754085.

[14] H. Myalska, K. Szymański, and G. Moskal, "Microstructure and properties of WC-Co HVAF coatings obtained from standard, superfine and modified by sub-micrometric carbide powders," *Arch. Metall. Mater.*, vol. 60, pp. 759–766, 2015, doi: 10.1515/amm-2015-0203.

[15] P.L. Fauchais, J.V.R. Heberlein, and M.I. Boulos, "*Thermal Spray Fundamentals: From Powder to Part*," Springer, New York, 2014.

[16] R. Szklarek *et al.*, "High temperature resistance of silicide-coated niobium," *Bull. Pol. Acad. Sci. Tech. Sci.*, vol. 69, no. 5, article number: e137416, 2021, doi: 10.24425/bpasts.2021.137416.

[17] W. Żórawski, M. Makrenek, and A. Góral, "Mechanical properties and corrosion resistance of HVOF sprayed coatings using nanostructured carbide powders," *Arch. Metall. Mater.*, vol. 61, pp. 1839–1846, 2016, doi: 10.1515/AMM-2016-0297.

[18] L.M. Berger, "Application of hardmetals as thermal spray coatings," *Int. J. Refract. Met. Hard Mater.*, vol. 49, pp. 350–364, 2015, doi: 10.1016/j.ijrmhm.2014.09.029.

[19] V. Singh *et al.*, "Cavitation erosion behavior of high velocity oxy fuel (HVOF) sprayed (VC + CuNi-Cr) based novel coatings on SS316 steel," *Surf. Coat. Technol.*, vol. 432, pp. 1–15, 2022, doi: 10.1016/j.surfcoat.2021.128052.

[20] R.S. Lima and B.R. Marple, "Thermal spray coatings engineered from nanostructured ceramic agglomerated powders for structural, thermal barrier and biomedical applications: A review," *J. Therm. Spray. Technol.*, vol. 16, pp. 40–63, 2007, doi: 10.1007/ s11666-006-9010-7.

[21] S. Houdkova, M. Kasparova, and F. Zahalka, "The Influence of Spraying Angle on Properties of HVOF Sprayed Hardmetal Coatings," *J. Therm. Spray. Technol.*, vol. 19, no. 5, pp. 893–901, doi: 2010, doi:10.1007/s11666-010-9514-z.

[22] A. Valarezo, K. Shinoda, and S. Sampath, "Effect of Deposition Rate and Deposition Temperature on Residual Stress of HVOF-Sprayed Coatings," *J. Therm. Spray. Technol.*, vol. 29, pp. 1322–1338, 2020, doi: 10.1007/s11666-020-01073-y.

[23] E. Jonda, L. Łatka, and W. Pakieła, "Comparison of Different Cermet Coatings Sprayed on Magnesium Alloy by HVOF," *Materials*, vol. 14, p. 1594, 2021, doi: 10.3390/ma14071594.

[24] E. Jonda, and L. Łatka, "Comparative Analysis of Mechanical Properties of WC-Based Cermet Coatings Sprayed by HVOF onto AZ31 Magnesium Alloy Substrates," *Adv. Sci. Technol. Res. J.*, vol. 15, no. 2, pp. 57–64, 2021, doi: 10.12913/22998624/135979.

[25] A. Aguero *et al.*, "HVOF-deposited WCCoCr as replacement for hard Cr in landing gear actuators," *J. Therm. Spray Technol.*, vol. 20, pp.1292–309, 2011, doi: 10.1007/s11666-011-9686-1.

[26] P. Komarov, D. Jech, S. Thachenko, K. Slamecka, K. Dvorak, and L. Celko, "Wetting Behavior of Wear-Resistant WC-Co–Cr Cermet Coatings Produced by HVOF: The Role of Chemical Composition and Surface Roughness," *J. Therm. Spray Technol.*, vol. 30, pp. 285–303, 2021, doi: 10.1007/s11666-020-01130-6.

[27] X. Ding, D. Ke, C. Yuan, Z. Ding, and X. Cheng, "Microstructure and cavitation erosion resistance of HVOF deposited WC-Co coatings with different sized WC," *Coatings*, vol. 8, no. 307, p. 307, 2018, doi: 10.3390/coatings8090307.

[28] W. Tillmann, S. Kuhnt, I.T. Baumann, A. Kalka, E.-C. Becker-Emden, and A. Brinkhoff, "Statistical Comparison of Processing Different Powder Feedstock in an HVOF Thermal Spray Process," *J. Therm. Spray Technol.*, vol. 31, pp. 1476–1489, 2022, doi: 10.1007/s11666-022-01392-2.

[29] H. Wang, Q. Qiu, M. Gee, C. Hou, X. Liu, and X. Song, "Wear resistance enhancement of HVOF-sprayed WC-Co coating by complete densification of starting powder," *Mater. Des.*, vol. 191, p. 108586, 2020, doi: 10.1016/j.matdes.2020.108586.

[30] B. Song, J.W. Murray, R.G. Wellman, Z. Pala, and T. Hussain, "Dry sliding wear behaviour of HVOF thermal sprayed WC-Co–Cr and WC-CrxCy-Ni coatings," *Wear*, vol. 442–443, p. 203114, 2020, doi: 10.1016/j.wear.2019.203114.

[31] M. Górnik, E. Jonda, L. Łatka, M. Nowakowska, and M. Godzierz, "Influence of spray distance on mechanical and tribological properties of HVOF sprayed WC-Co–Cr coatings," *Mat. Sci. Pol.*, vol. 39, no. 4, pp. 545–554, 2021, doi: 10.12913/22998624/135979.

[32] L.A. Luiz *et al.*, "Corrosion Behavior and Galvanic Corrosion Resistance of WC and Cr_3C_2 Cermet Coatings in Madeira River Water," *J. Therm. Spray Techn.*, vol. 30, pp. 205–221, 2021, doi: 10.1007/s11666-021-01152-8.

[33] L. Qiao, Y. Wu, S. Hong, W. Long, and J. Cheng, "Wet abrasive wear behavior of WC-based cermet coatings prepared by HVOF spraying," *Ceram. Int*., vol. 47, no. 2, pp. 1829–1836, 2021, doi: 10.1016/j.ceramint.2020.09.009.

[34] A. Raza, F. Ahmad, T.M. Badri, M.R. Raza, and K. Malik, "An Influence of Oxygen Flow Rate and Spray Distance on the Porosity of HVOF Coating and Its Effects on Corrosion – A Review," *Materials*, vol. 15 6329, 2022, doi: 10.3390/ma15186329.

[35] V. Testa, S. Morelli, G. Bolelli, B. Benedetti, P. Puddu, P. Sassatelli, and L. Lusvarghi, "Alternative metallic matrices for WC-based HVOF coatings," *Surf. Coat. Technol.*, vol. 402, p. 126308, 2020, doi: 10.1016/j.surfcoat.2020.126308.

[36] H. Myalska, L. Lusvarghi, G. Bolelli, P. Sassatelli, and G. Moskal, "Tribological behavior of WC-Co HVAF-sprayed composite coatings modified by nano-sized TiC addition," *Surf. Coat. Technol.*, vol. 371, pp. 401–416, 2019, doi: 10.1016/j.surfcoat.2018.09.017.

[37] C. Verdon, A. Karimi and J.-L. Martin, "A study of high velocity oxy-fuel thermally sprayed tungsten carbide based coatings. Part 1: Microstructures," *Mater. Sci. Eng. A*, vol. 246, no. 1–2, pp. 11–24, 1998, doi: 10.1016/S0921-5093(97)00759-4.

[38] Y.Y. Santana *et al.*, "Characterization and residual stresses of WC-Co thermally sprayed coatings," *Surf. Coat. Technol.*, vol. 202, no. 18, pp. 4560–4565, 2008, doi: 10.1016/j.surfcoat.2008.04.042.

[39] C. Bartuli, T. Valente, F. Cipri, E. Bemporad, and M. Tului, "Parametric study of an HVOF process for the deposition of nanostructured WC-Co coatings," *J. Therm. Spray Technnol.*, vol. 14, pp. 187–95, 2005, doi: 10.1361/10599630523746.

[40] J.A. Picas, E. Ruperez, M. Punset, and A. Forn, "Influence of HVOF spraying parameters on the corrosion resistance of WC-CoCr coatings in strong acidic environment," *Surf. Coat. Technol.*, 225:47-57, 2013, doi: 10.1016/J.SURFCOAT.2013.03.015.

[41] G. Bolelli *et al.*, "Tribology of HVOF- and HVAF-sprayed WC – 10Co4Cr hardmetal coatings: A comparative assessment," *Surf. Coat Technol.*, vol. 265, pp. 125–144, 2015, doi: 10.1016/J.SURFCOAT.2015.01.048.

[42] M.M. Lachowicz and M. Winnicki, "Corrosion Damage Mechanisms of TiO_2 Cold-Sprayed Coatings," *Arch. Metall. Mater.*, vol. 67, pp. 975–985, 2022, doi: 10.24425/amm.2022.139691.

[43] M.A. Osipenko, D.S. Kharytonau, A.A. Kasach, J. Ryl, J. Adamiec, and I.I. Kurilo, "Inhibitive effect of sodium molybdate on corrosion of AZ31 magnesium alloy in chloride solutions," *Electrochem. Acta.*, vol. 414, p. 140175, 2022, doi: 10.1016/j.electacta.2022.140175.

[44] X. Fang, J. Yang, S. Wang, C. Wang, K. Huang, H. Li, and B. Lu, "Additive manufacturing of high performance AZ31 magnesium alloy with full equiaxed grains: Microstructure, mechanical property, and electromechanical corrosion performance," *J. Therm. Spray Technol.*, vol. 300, pp. 117430, 2022, doi: 10.1016/j.jmatprotect.2021.117430.

[45] R. Xu, D. Jiang, Y. Zhou, X. Lu, T. Zhang, and F. Wang, "Influence of 2,6-dihydroxybenzoic acid on the corrosion behavior and discharge performance of AZ31 Mg alloy," *Vacuum*, vol. 200, p. 111031, 2022, doi: 10.1016/j.vacuum.2022.111031.

[46] D. Utu, I. Hulka, V.A. Serban and H. Filipescu. "Corrosion properties of cermet coatings sprayed by high-velocity-oxygen-fuel," *4th International Conference NANOCON 2012*, Czech Republic, 2021, pp. 520–525.

[47] S. Shabana, M.M.M. Sarcar, K.N.S. Suman, and S. Kamaluddin, "Tribological and corrosion behavior of HVOF Sprayed WC-Co, NiCrBSi and Cr_3C_2-NiCr Coatings and analysis using Design of Experiments," *Mater. Today. Proc.*, vol. 2, no. 4–5, pp. 2654–2665, 2015, doi: 10.1016/j.matpr.2015.07.227.

[48] S. Hong *et al.*, "Effect of Spray Parameters on the Corrosion Behavior of HVOF Sprayed WC-Co–Cr Coatings," *J. Mater. Eng. Perform.*, vol. 23, pp. 1434–1439, 2014, doi: 10.1007/s11665-014-0865-3.

[49] J.M. Perry, T. Hodgkiess, and A. Neville, "A Comparison of the Corrosion Behavior of WC-Co–Cr and WC-Co HVOF Thermally Sprayed Coatings by In Situ Atomic Force Microscopy (AFM)," *J. Therm. Spray Technol.*, vol. 11, pp. 536–541, 2002, doi: 10.1361/105996302770348673.

[50] V. Testa *et al.*, "Corrosion and wear performances of alternative TiC-based thermal spray coatings," *Surf. Coat. Technol.*, vol. 438, p. 128400, 2022, doi: 10.1016/j.surfcoat.2022.128400.

[51] L.-M. Berger, S. Saaro, T. Naumann, M. Kašparova, and F. Zahálka, "Influence of feedstock powder characteristics and spray processes on microstructure and properties of WC–(W,Cr)2C–Ni hardmetal coatings," *Surf. Coat. Technol.*, vol. 205, pp. 1080–1087, 2010, doi: 10.1016/j.surfcoat.2010.07.032.

[52] U. Selvadurai *et al.*,, "Influence of the handling parameters on residual stresses of HVOF-sprayed WC-12Co coatings," *Surf. Coat. Technol.*, vol. 268, pp. 30–35, 2015, doi: 10.1016/j.surfcoat.2014.11.055.

[53] H.S. Sidhu, B.S. Sidhu, and S. Prakash, "Mechanical and microstructural properties of HVOF sprayed WC-Co and Cr_3C_2-NiCr coatings on the boiler tube steels using LPG as the fuel gas," *J. Mater. Process. Technol.*, vol. 171, no. 1, pp. 77–82, 2006, doi: 10.1016/j.jmatprotec.2005.06.058.

[54] A.C. Karaoglanli, M. Oge, K.M. Doleker, and M. Hotamis, "Comparison of tribological properties of HVOF sprayed coatings with different composition," *Surf. Coat. Technol.*, vol. 318, pp. 299–308, 2017, doi: 10.1016/j.surfcowat.2017.02.021.

[55] S. Houdkova, O. Blahova, F. Zahalka, and M. Kasparova, "The instrumented indentation study of HVOF sprayed hardmetal coatings," *J. Therm. Spray Technol.*, vol. 21, no. 1, pp. 77–85, 2012, doi: 10.1007/s11666-011-9677-2.

[56] G. Bolelli, L-M. Berger, M. Bonetti, and L. Lusvarghi, "Comparative study of the dry sliding wear behaviour of HVOF-sprayed WC-(W,Cr)2C–Ni and WC-CoCr hard metal coatings," *Wear*, vol. 309, no. 1–2, pp. 96–111, 2014, doi: 10.1016/j.wear.2013.11.001.